# Biobased Multifunctional Ingredients for Manufacturing Tire Tread with High Mechanical Strength and Fuel-Saving Efficiency

Mingxu Wu[a,b], Xin He[a,b], Songbo Zhang[b,c]*, Qizhou Yu[b,c], Pibo Liu[b,c], Shuwei Wang[a]*, Yanming Hu[b,c]*

[a] School of Textile and Material Engineering, Dalian Polytechnic University, Dalian 116034, China

[b] Division of Energy Materials, Dalian Institute of Chemical Physics, Chinese Academy of Sciences, Dalian 116023, China

[c] Liaoning Key Laboratory of Specialty Polymers, Dalian 116023, China

*Corresponding authors: Songbo Zhang (zhangsongbo@dicp.ac.cn), Shuwei Wang (wangshuwei@dlpu.edu.cn), and Yanming Hu (ymhu@dicp.ac.cn)

**Table S1.** Formulations for SSBR/CB composites [a]

| Samples | SSBR | AO | Poly($S_{30}EO_{70}$) | Poly($S_{30}ER_{70}$) | Poly($S_{30}OA_{70}$) | Poly($S_{30}RA_{70}$) |
|---|---|---|---|---|---|---|
| SSBR/AO | 100 | 5 | 0 | 0 | 0 | 0 |
| SSBR/poly($S_{30}$-$EO_{70}$) | 100 | 0 | 5 | 0 | 0 | 0 |
| SSBR/poly($S_{30}$-$ER_{70}$) | 100 | 0 | 0 | 5 | 0 | 0 |
| SSBR/poly($S_{30}$-$OA_{70}$) | 100 | 0 | 0 | 0 | 5 | 0 |
| SSBR/poly($S_{30}$-$RA_{70}$) | 100 | 0 | 0 | 0 | 0 | 5 |

[a] The unit is phr (parts per hundred parts of rubber), and other additives are as follows, ZnO: 5 phr; SA: 2 phr; 4010NA:2 phr; CB: 50 phr; CBS:1.5phr; MBTS:0.5phr; S:1.5phr.

**Table S2.** Formulations for tread composites [a].

| Samples | SSBR | BIR | BR | AO | ER | Poly($S_{30}$-$ER_{70}$) |
|---|---|---|---|---|---|---|
| BR-Tread/AO | 80 | 0 | 20 | 5 | 0 | 0 |
| BR-Tread/poly($S_{30}$-$ER_{70}$) | 80 | 0 | 20 | 0 | 0 | 5 |
| Tread/AO | 80 | 20 | 0 | 5 | 0 | 0 |
| Tread/ER | 80 | 20 | 0 | 0 | 5 | |
| Tread/poly($S_{30}$-$ER_{70}$) | 80 | 20 | 0 | 0 | 0 | 5 |

[a] Other additives are as follows, ZnO: 3 phr; SA: 2 phr; 4010NA:2 phr; CB: 50 phr; TBBS:0.7 phr; S:1.0 phr.

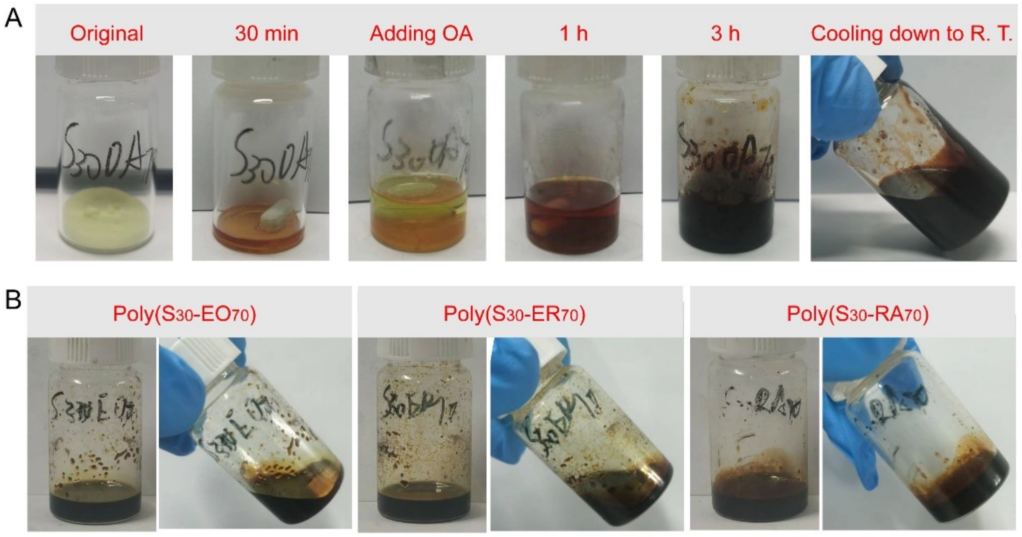

**Fig. S1**. (A) Polymerization phenomena for poly($S_{30}$-$OA_{70}$) and (B) appearances of poly($S_{30}$-$EO_{70}$), poly($S_{30}$-$ER_{70}$) and poly($S_{30}$-$RA_{70}$).

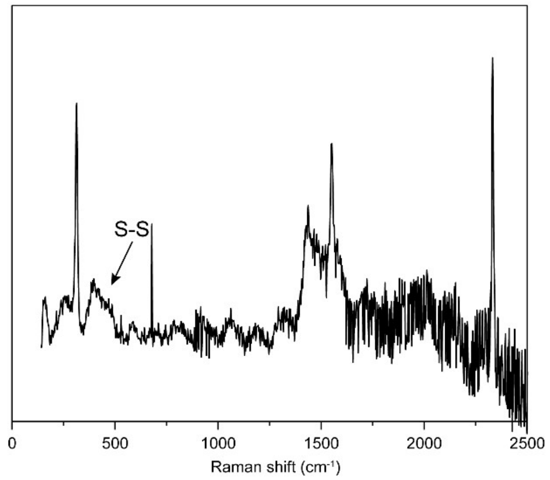

**Fig. S2**. Raman spectrum of poly($S_{30}$-$OA_{70}$) under 355nm excitation wavelength.

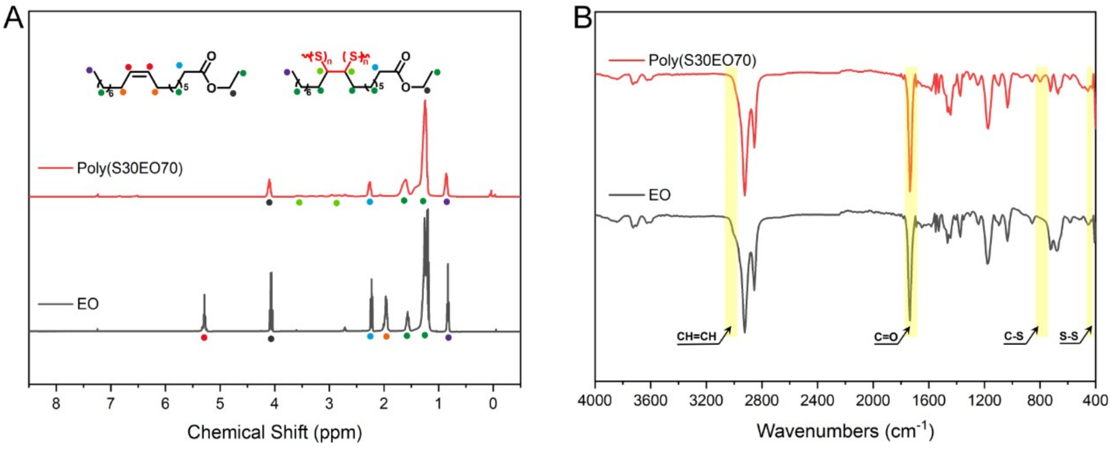

**Fig. S3.** (A) $^1$H NMR and (B) FT-IR spectroscopies of EO and poly($S_{30}$-$EO_{70}$).

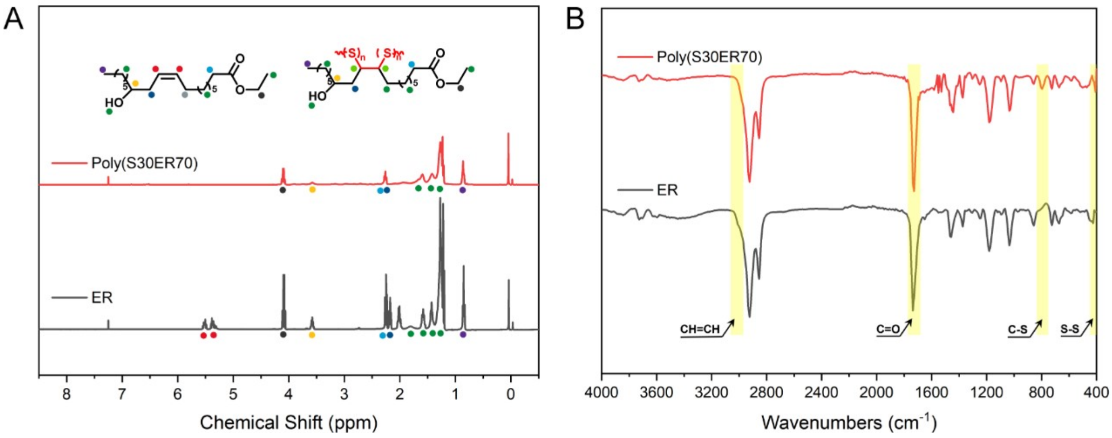

**Fig. S4.** (A) $^1$H NMR and (B) FT-IR spectroscopies of ER and poly($S_{30}$-$ER_{70}$).

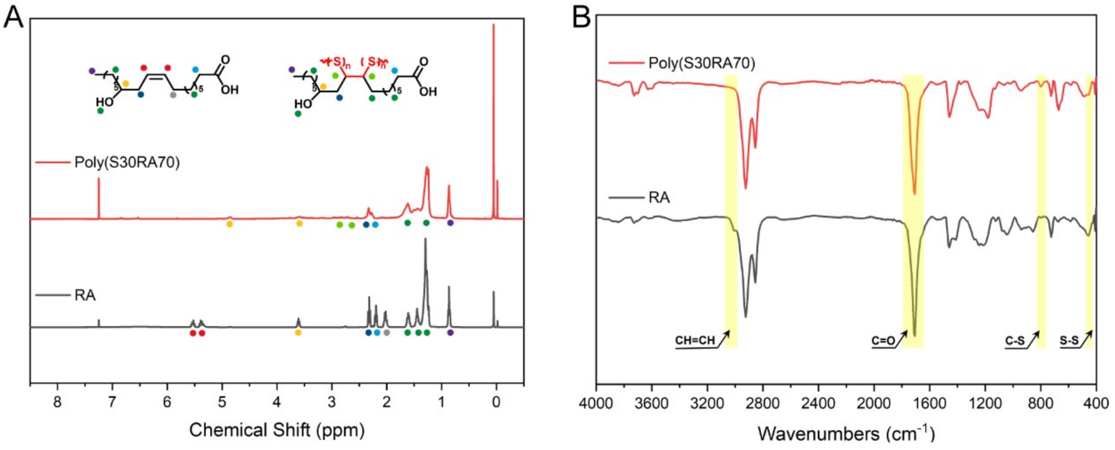

**Fig. S5.** (A) $^1$H NMR and (B) FT-IR spectroscopies of RA and poly($S_{30}$-$RA_{70}$).

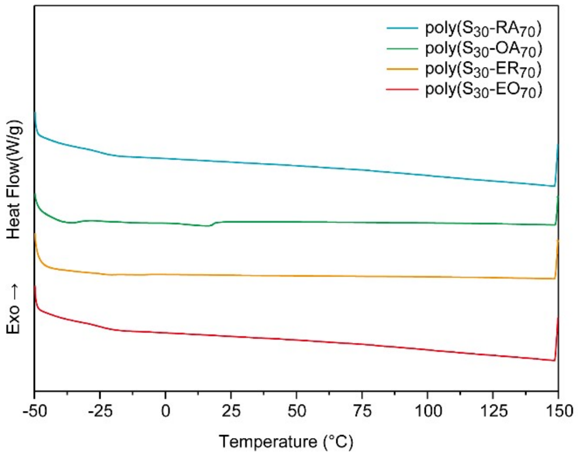

**Fig. S6.** DSC curves of the as-synthesized sulfur-rich copolymers.

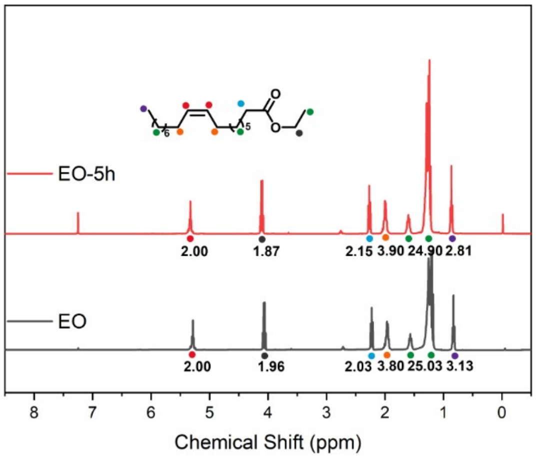

**Fig. S7.** $^1$H NMR spectra of EO before and after heating under the same condition as preparation of poly($S_{30}$-$EO_{70}$).

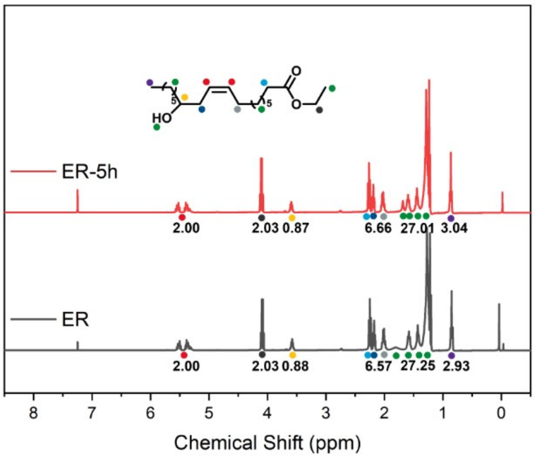

**Fig. S8.** $^1$H NMR spectra of ER before and after heating under the same condition as preparation of poly($S_{30}$-$ER_{70}$).

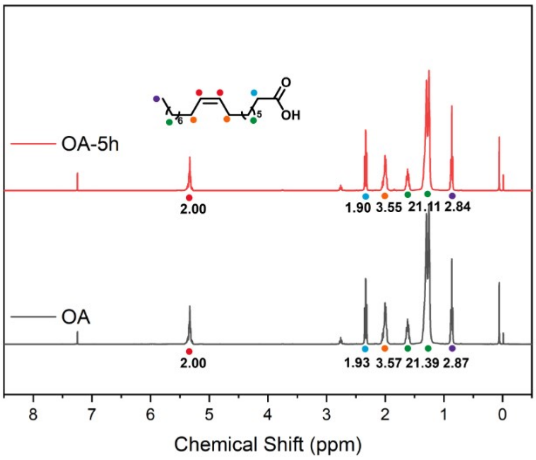

**Fig. S9.** $^1$H NMR spectra of OA before and after heating under the same condition as preparation of poly($S_{30}$-$OA_{70}$).

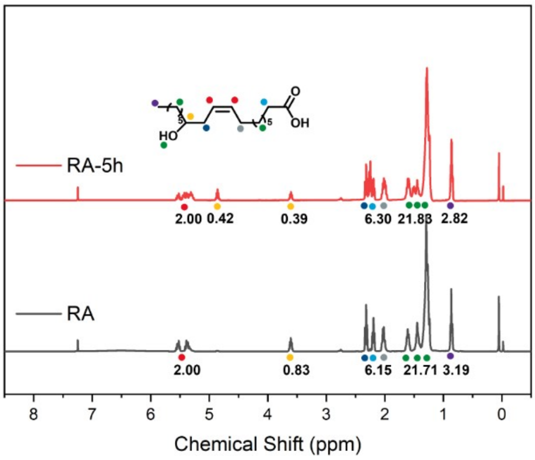

**Fig. S10.** $^1$H NMR spectra of RA before and after heating under the same condition as preparation of poly($S_{30}$-$RA_{70}$).

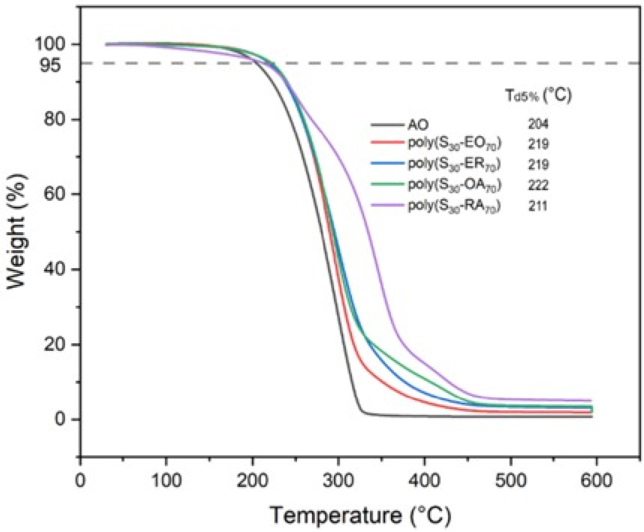

**Fig. S11.** TGA curves of AO, poly($S_{30}$-$EO_{70}$), poly($S_{30}$-$ER_{70}$), poly($S_{30}$-$OA_{70}$) and poly($S_{30}$-$RA_{70}$).

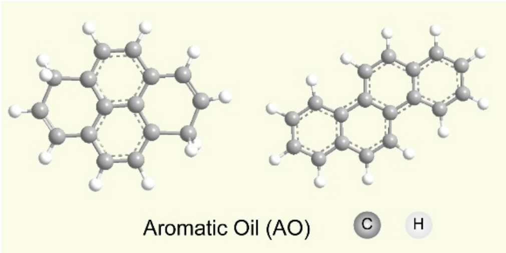

**Fig. S12.** Optimized molecular geometry of aromatic oil (AO).

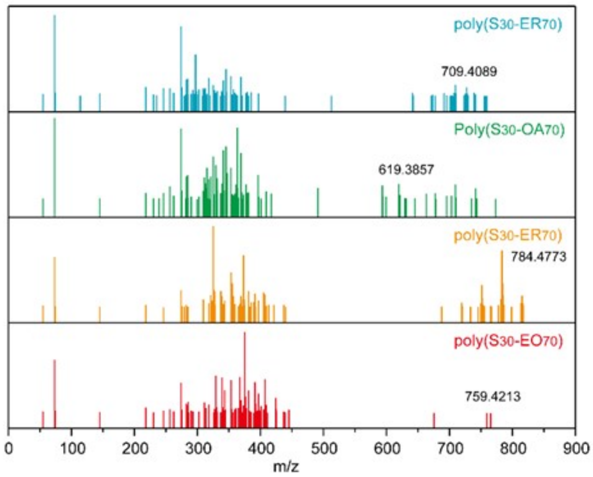

**Fig. S13**. LC-MS results of poly($S_{30}$-$EO_{70}$), poly($S_{30}$-$ER_{70}$), poly($S_{30}$-$OA_{70}$) and poly($S_{30}$-$RA_{70}$).

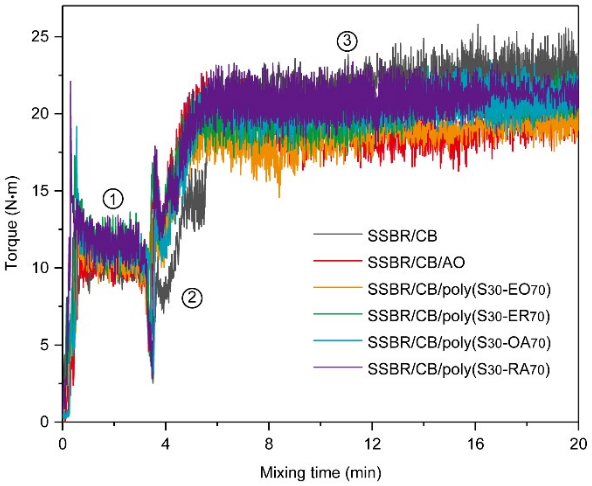

**Fig. S14**. Torque evolution during the mixing of SSBR compounds. ① SSBR is charged and masticated; ② CB and plasticizer are added, and ③ all ingredients are mixed.

**Table S3.** Curing parameters of SSBR/CB composites.

| Samples | $t_{s1}$(m:s)[a] | $t_{90}$(m:s) | $M_L$ (N·m) | $M_H$ (N·m) | ΔM (N·m)[b] |
|---|---|---|---|---|---|
| SSBR/AO | 4:02 | 26:43 | 0.19 | 1.41 | 1.22 |
| SSBR/poly($S_{30}$-$EO_{70}$) | 3:13 | 29:24 | 0.21 | 1.52 | 1.31 |
| SSBR/poly($S_{30}$-$ER_{70}$) | 2:52 | 29.49 | 0.20 | 1.46 | 1.26 |
| SSBR/poly($S_{30}$-$OA_{70}$) | 2:56 | 34:51 | 0.24 | 1.92 | 1.68 |
| SSBR/poly($S_{30}$-$RA_{70}$) | 2:38 | 31:31 | 0.33 | 2.11 | 1.78 |

[a] m:s is the abbreviation of (minute:second). [b] ΔM was defined as the torque difference between the maximum torque ($M_H$) and minimum torque ($M_L$).

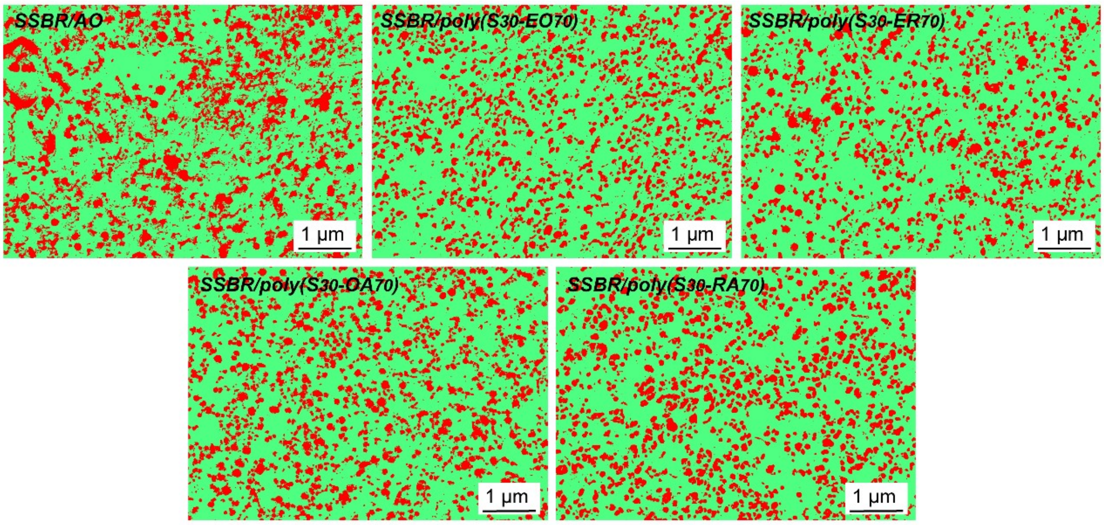

**Fig. S15** Processing images of Figs. 4A – 4E by ImageJ software.

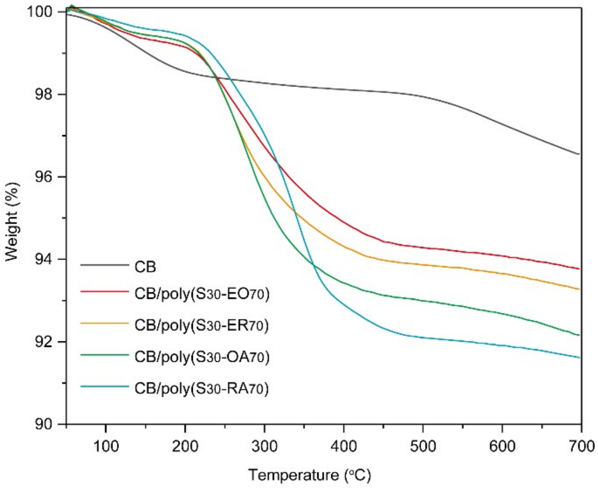

**Fig. S16**. TGA profiles for CB and SP-grafted CB.

As shown in **Fig. S16**, compared with pristine CB (2.7%), the SP-grafted CBs have a larger mass loss between 130 and 700 °C, especially 5.7% for poly($S_{30}$-$EO_{70}$), 6.2% for poly($S_{30}$-$ER_{70}$), 7.4% for poly($S_{30}$-$OA_{70}$) and 8.1% for poly($S_{30}$-$RA_{70}$), owing to the decomposition of the grafted sulfur-rich polymer (SP). The grafting efficiency can be calculated by the following equation.

$$\text{grafting efficiency} = \frac{W_2 - W_1}{1 - (W_2 - W_1)} \times \frac{m_{CB}}{m_{SP}} \times 100\%$$

where $W_1$ and $W_2$ represent the mass loss of pristine carbon black (CB) and SP-modified carbon black ranging from 130°C to 700°C, respectively (%), respectively; $m_{CB}$ and $m_{sp}$ denote the feeding weights of CB (10.0 g) and SP (1.0 g) in the preparation of SP-modified CB, respectively. Accordingly, the grafting efficiency of poly($S_{30}$-$RA_{70}$) and poly($S_{30}$-$OA_{70}$) toward CB are calculated to be 56.4% and 48.8%, higher than that of 30.7% for poly($S_{30}$-$EO_{70}$) and 36.6% for poly($S_{30}$-$ER_{70}$). It is likely due to a higher reactivity between carbonyl group and CB than ester group and hydrogen group as well as multiple reactive sites in poly($S_{30}$-$RA_{70}$).

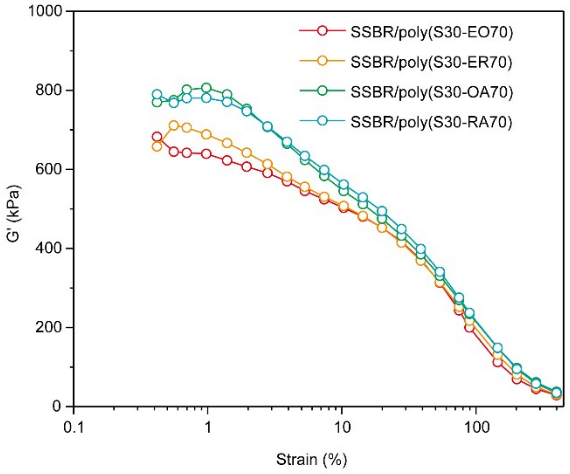

**Fig. S17.** Payne effect of the SSBR/poly($S_{30}$-$EO_{70}$), SSBR/poly($S_{30}$-$ER_{70}$), SSBR/poly($S_{30}$-$OA_{70}$), and SSBR/poly($S_{30}$-$RA_{70}$) compounds.

The storage modulus G′ under oscillatory shear strain for SSBR/poly($S_{30}$-$EO_{70}$), SSBR/poly($S_{30}$-$ER_{70}$), SSBR/poly($S_{30}$-$OA_{70}$), and SSBR/poly($S_{30}$-$RA_{70}$) were investigated using a rubber process analyzer (RPA), as shown in **Fig. S17**. Clearly, the storage modulus G’ for all SPs-based SSBR compounds collapses to a minimum value with the applied strain increasing, suggesting the breakdown of CB network. In plasticizer-based systems, the ΔG′ parameter fundamentally serves as a dual-function indicator, simultaneously reflecting filler dispersion characteristics and quantifying plasticization efficacy [1]. Given the well-dispersed carbon black (CB) in the rubber matrix (**Fig. 3**), indicative of weak CB network interactions, the observed ΔG′ predominantly arise from two mechanisms: the plasticization effect of SPs and the interfacial interactions between polar groups in SPs and CB. Consistent with the results that the minimum torque (ΔL, **Table S1**) and the processing characteristics (**Fig. S14**), the SSBR/poly($S_{30}$-$OA_{70}$) and SSBR/poly($S_{30}$-$RA_{70}$) systems exhibited higher ΔG′ values compared to SSBR/poly($S_{30}$-$EO_{70}$) and SSBR/poly($S_{30}$-$ER_{70}$) systems (768.9 kPa vs. 755.0 kPa vs. 653.8 kPa vs. 680.3 kPa).

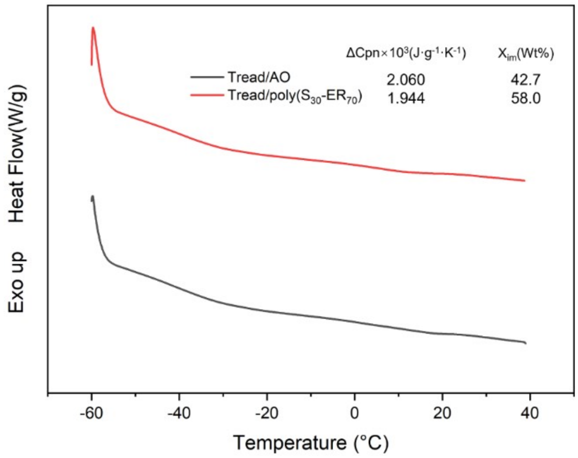

**Fig. S18.** DSC curves of the glass transition region of tread compounds.

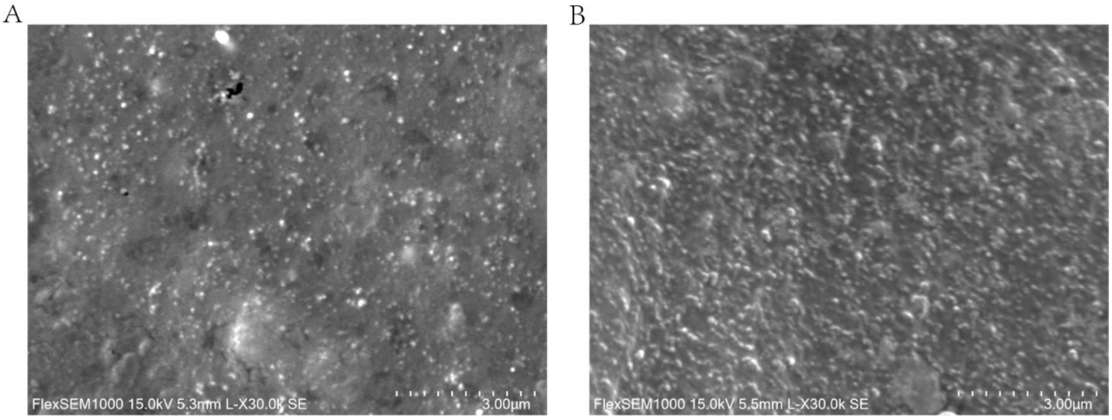

**Fig. S19.** SEM images of (A) tread/AO and (B) tread/poly($S_{30}$-$ER_{70}$) composites.

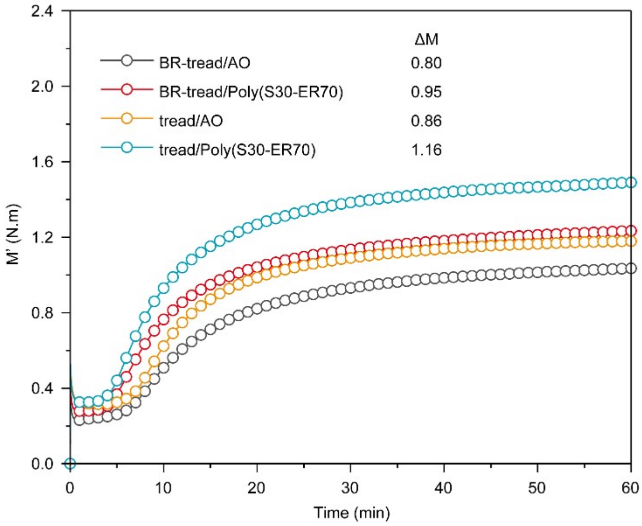

**Fig. S20.** Curing curves of tread/AO and tread/poly($S_{30}$-$ER_{70}$) composites.

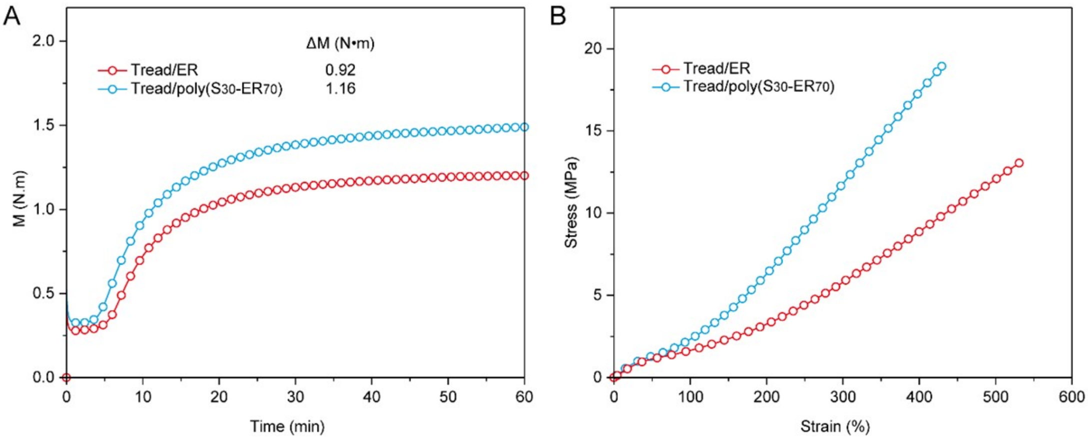

**Fig. S21**. (A) Curing curves and (B) stress-strain curves of tread/ER and tread/Poly($S_{30}$-$ER_{70}$) composites.

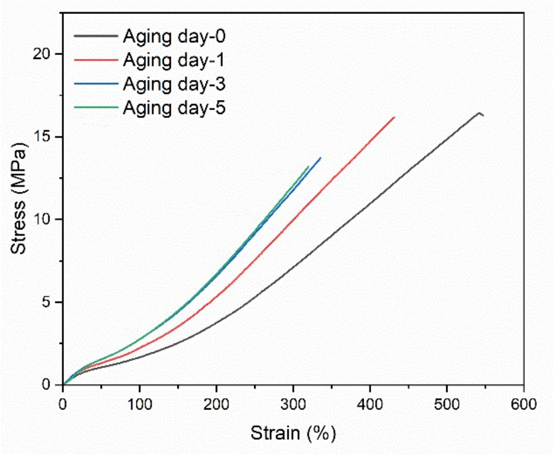

**Fig. S22.** Stress-strain curves of tread/AO composites under different aging days.

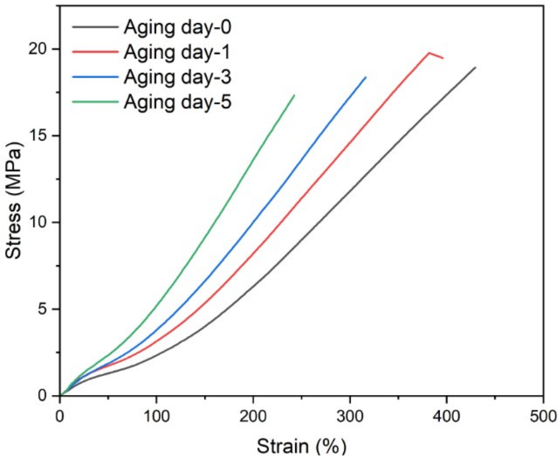

**Fig. S23.** Stress-strain curves of tread/poly($S_{30}$-$ER_{70}$) composites under different aging days.

**Table S4.** The mechanical propeties of tread compoites under different aging days.

| Samples | | TS (MPa) | EB (%) |
|---|---|---|---|
| Tread/AO | Aging day-0 | 16.4±0.4 | 542±18 |
| | Aging day-1 | 16.2±0.7 | 431±15 |
| | Aging day-3 | 13.7±0.3 | 336±9 |
| | Aging day-5 | 13.2±0.4 | 319±15 |
| Tread/poly($S_{30}$-$ER_{70}$) | Aging day-0 | 18.9±0.5 | 429±10 |
| | Aging day-1 | 19.8±0.7 | 382±13 |
| | Aging day-3 | 18.4±0.2 | 316±12 |

|  |  |  |  |
|---|---|---|---|
|  | Aging day-5 | 17.3±0.5 | 242±7 |

**Table S5**. Formulation for the SSBR/BIR sample.[a]

| Code | SSBR | BIR | ZnO | SA | 4010NA | TBBS | Poly($S_{30}$-$ER_{70}$) |
|---|---|---|---|---|---|---|---|
| SSBR/BIR | 80 | 20 | 3 | 2 | 2 | 0.7 | 5 |

[a] The sample was prepared using a two-stage vulcanization method as follows: first stage: 150 °C × $t_{90}$ × 12.5 MPa, and second stage: 150 °C × 30 min × 12.5 MPa.

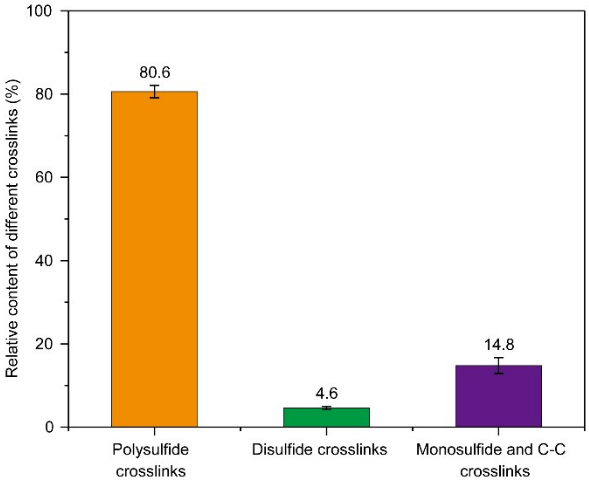

**Fig. S24.** Different crosslinks content in poly($S_{30}$-$EO_{70}$)-based SSBR/BIR vulcanizate.

## Reference

1. F. van Elburg, F. Grunert, C. Aurisicchio, M. di Consiglio, R. di Ronza, A. Talma, P. Bernal-Ortega and A. Blume, *Polymers*, 2024, **16**, 1880.